Ball milling-induced reduction of MoS₂ with Al

L. Takacs · P. Baláž · A. R. Torosyan

Abstract The ball milling-induced reduction of MoS₂ by Al has been investigated. Although this is a highly exothermic reaction that, based on its thermodynamic properties, should progress as a self-sustaining process, ignition could not be achieved by ball milling. In order to identify the reason, XRD, particle size distribution, SEM, and DTA measurements were carried out on a series of samples milled for different durations. It was found that the largest composite agglomerates broke up due to the presence of a fine dispersion of MoS₂ particles. SEM also revealed that the grains are packed rather loosely within the agglomerates. These results indicate that a self-sustaining process can take place only if large and well-compacted composite particles are present.

Introduction

Ball milling-induced chemical reactions and alloying have been the subjects of numerous investigations [1–3]. In particular, displacement reactions between a metal compound (oxide, chalcogenide, halide) and a reducing metal attracted significant attention, because they are convenient model reactions [4–6] and also because they provide the basis of several possible applications. For example, nanocrystalline dispersoids were created by in situ displacement reactions in aluminum matrix [7]; rare earth metals were refined by milling their oxide or chloride with Ca or Na [8]; and free nanocrystalline metal powders were prepared by the mechanochemical reduction of their halides [9]. If the reaction is highly exothermic, the impact of the milling balls can initiate mechanically induced self-sustaining reaction (MSR) [10–12]. The ignition of MSR takes place after a certain activation time, during which the powder mixture reaches a critical state due to the physical and chemical changes caused by ball milling [4, 12, 13].

Typically, a reaction can propagate in the form of a self-sustaining process, if $\Delta H/C$, the magnitude of the reaction heat divided by the room temperature heat capacity of the product, is higher than about 2,000 K [12]. This "rule of thumb" applies to both MSR and thermally ignited self-propagating high temperature synthesis (SHS) [14]. The reduction of MoS₂ by Al takes place according to the equation

$$3MoS_2 + 4Al = 3Mo + 2Al_2S_3 - \Delta H \qquad (1)$$

where the value of $\Delta H/C$ is 2,093 K (The thermochemical properties were taken from Ref. [15]). Therefore, the initiation of MSR is anticipated, when ball milling is carried out on a stoichiometric mixture of MoS₂ and Al powders. Expecting MSR in this system is also reasonable because it was observed in similar displacement

L. Takacs (✉)
Department of Physics, University of Maryland, Baltimore County, 1000 Hilltop Circle, Baltimore, MD 21250, USA
e-mail: takacs@umbc.edu

P. Baláž
Institute of Geotechnics, Slovak Academy of Sciences, Watsonova 45, 043 53 Kosice, Slovakia

A. R. Torosyan
Institute of General and Inorganic Chemistry, National Academy of Science, 2-tup, 10 Argutyan Street, Yerevan 375051, Armenia

reactions with somewhat lower values of $\Delta H/C$. For example, milling CuO with Fe ($\Delta H/C$ = 1,850 K) [4] and Cu$_2$O with Zn ($\Delta H/C$ = 1,990 K) (Takacs, unpublished result) resulted in the ignition of MSR, if appropriate processing conditions were chosen. When $\Delta H/C$ is much lower, such as for the reduction of Fe$_3$O$_4$ with Zn ($\Delta H/C$ = 1,240 K) the reaction always takes place gradually, often with the formation of intermediate mixed phases [5].

Although the gradual versus self-sustaining nature of a mechanochemical reaction depends primarily on the exothermicity of the process, it is certainly not the only factor influencing reaction kinetics. For example, self-sustaining displacement reactions using Zr as the reducing metal start after much shorter activation times than similar reactions with either Ti or Hf, due to the faster diffusion of oxygen in ZrO$_2$ compared to TiO$_2$ and HfO$_2$ [6]. The mechanical properties of the powder are also important, as they influence the milling efficiency and the microstructure of the particles. MoS$_2$ is of interest in this respect, because it acts as a dry lubricant due to its layered atomic structure. Its crystals are built of sheets formed by a layer of Mo atoms sandwiched between two layers of S atoms. The sheets are held together by weak van der Waals forces, resulting in the graphite-like behavior of MoS$_2$. The objective of this investigation is to explore how the unique properties of MoS$_2$ effect its mechanochemical reduction with Al. Preliminary studies have shown that MSR is not possible in spite of the high value of $\Delta H/C$. Consequently, the main goal of this investigation is to find out exactly what prevents the ignition of MSR in this sufficiently exothermic system.

Experimental

The starting materials were MoS$_2$ (99.0%) and Al (99.5%, 325 mesh) powders obtained from AlfaÆsar. The stoichiometry of the starting mixtures corresponded to Eq.1. Attempts to induce MSR by ball milling were carried out using a SPEX 8000 Mixer Mill and round- and flat-ended hardened steel vials with several combinations of steel balls, 12.7, 9.5, and 6.3 mm in diameter. The temperature of the milling vial was recorded using a K-type thermocouple connected to a data-logging system. The ignition of MSR could be noticed from the resulting abrupt increase of the temperature as it was done in the case of other MSRs [12]. A series of samples milled for different durations was prepared by processing 3 g of powder with a combination of two 12.7-mm and five 9.5-mm balls (corresponding to a ball-to-powder mass ratio of about 12:1).

XRD measurements were performed using a Philips X'Pert diffractometer in Θ–Θ geometry with Cu–Kα radiation. The XRD lines were identified using the JCPDS database. The presented XRD patterns contain both the Kα_1 and Kα_2 contributions. For line width analysis, the Kα_2 sub-peaks were removed numerically.

The particle size distribution was measured by laser beam scattering using a Helos and Rodos granulometer (Sympatec, Germany). The uniform dispersion of the powders was assured by sonication for 1 min. SEM observations of the powder morphology were performed using a JEOL JSM-5600 scanning electron microscope. Both the external morphology of some powder particles sprinkled on conductive paint and the cross section of particles molded in epoxy were studied.

Thermal investigations were carried out using a Shimadzu DTA-50 high temperature differential thermal analyzer and flowing argon atmosphere.

Results and discussion

Searching for MSR

Based on the high value of $\Delta H/C$, the reduction of MoS$_2$ with Al was expected to take place as an MSR. Therefore, the temperature of the vial was measured during the milling process in order to detect the sudden heat release caused by ignition. However, the variation of the temperature was always smooth, showing only a gradual increase due to the steady input of mechanical energy. Several milling conditions were tried, from relatively mild (six 9.5-mm plus six 6.3-mm balls and round ended vial) to much more energetic (ten 12.7-mm balls and flat ended vial). In some experiments, the milling container was closed in a fiberglass glove box flushed with argon; other samples were prepared in air. Usually a 3-g batch of stoichiometric powder mixture was milled, but larger charges and a slight excess of Al were also tested. No ignition could be achieved under any of the applied conditions. Therefore, the reduction of MoS$_2$ with Al is probably always a gradual process, although the possibility of initiating MSR under different conditions cannot be excluded with absolute certainty.

Mechanochemical reactions begin with an initial period during which size reduction, mixing, and mechanical activation take place but little chemical transformation occurs. This activation period may last for a few seconds or several hours, depending on the system and the processing conditions. XRD was performed on the milled powder after every attempt to induce MSR in order to make sure that the process

was not interrupted too early. In each case, a large fraction of the powder was already transformed into the product phases by gradual reaction. As the product phases decrease $\Delta H/C$ and also reduce the contact area between the reactants, continued milling of the investigated powders could not bring about ignition.

Time dependence of the phase composition

Once the gradual nature of the reaction was established, a series of samples was prepared, milled for periods from 3 min to 120 min. In each case, 3 g of stoichiometric powder mixture was milled with two 12.7-mm and five 9.5-mm balls in a flat-ended vial, closed in air.

XRD was measured on each sample in order to establish the evolution of the phase composition. A few representative spectra are shown in Fig. 1. The relatively narrow angle range was chosen to demonstrate the main features of the process with good resolution. The actual measurements were taken from 8° to 80°. The patterns are dominated by the lines of the Mo-containing phases due to the high atomic number of Mo.

Close to the initial state (pattern A, milled for 3 min to ensure uniformity) the sample contains only the starting phases, MoS_2 and Al metal. The pattern of MoS_2 is indexed according to the equilibrium 2H stacking (JCPDS card 37-1492) although deviations from this structure are possible due to the layered nature of this compound. The only indication that deviations from the 2H form are actually present is the sub-peak on the high angle side of the (008) peak.
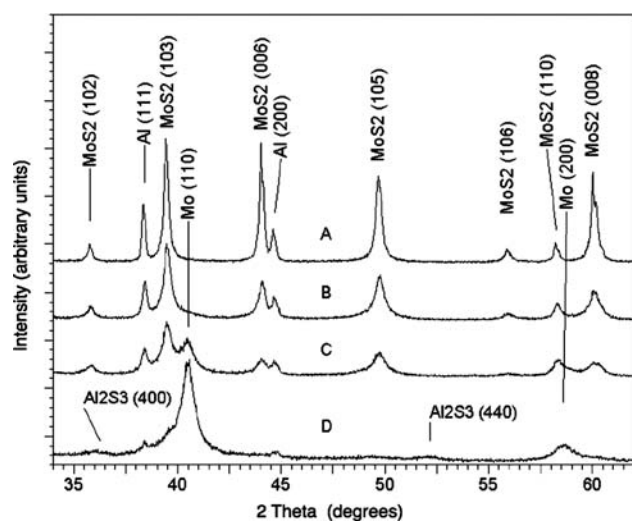
MoS_2 with 3R stacking (17-0744) has several lines in that angle range. As the powder is milled further, this sub-peak is no longer visible due to the broadening of the lines. A detailed investigation of the stacking of MoS_2 and its changes upon milling are beyond the scope of this investigation.

The only obvious change observed after 21 min of milling (pattern B) is the increase of the line widths. Significant chemical transformation begins only after this incubation time. After 34.5 min of milling (pattern C) a large fraction of the MoS_2 is reduced to Mo metal as shown by the emerging (110) peak. By 90 min (pattern D) the reaction is almost complete. The broad lines of nanocrystalline Mo dominate the spectrum and the most intense peaks of Al_2S_3 (26-0037) can be discerned. A very small amount of the initial phases is still present. (The presence of a small amount of Al metal also proves that oxidation was not a major problem in spite of handling the sample in air).

The intensity of an XRD peak is proportional to the amount of the corresponding phase. Yet, deriving quantitative reaction kinetics from the XRD spectra is a difficult matter, due to a number of additional factors influencing line intensities, such as absorption effects, overlap between the peaks, lattice defects, etc. Nevertheless, the semi-quantitative characterization of the reaction kinetics is often possible by calculating appropriate line intensity ratios. In this case, the only peak that is free from overlap over the entire sequence of spectra is the (105) peak of MoS_2. In order to minimize random intensity variations due to instrumental effects, the area of this peak was divided by the total area under the spectrum between 37.5° and 42.5°, where a combination of several peaks from different phases provide a reasonable measure of the overall intensity of the pattern. This intensity ratio was scaled to between one and zero to obtain the reactant fraction (Fig. 2.) Much of the decrease during the first 21 min of milling is probably an artifact related to defect formation. Nevertheless, the graph clearly shows that most of the reaction takes place between 20 min and 60 min and it is practically complete after 120 min of milling.

Particle size and microstructure

The XRD line widths provide information on the size of the coherently scattering domains and they also depend on the random lattice strain induced by milling. An attempt was made to separate the size and strain broadening contributions to the width of the MoS_2 peaks using the method of integral breadths [16]. The (002), (004), and the similarly oriented (105) peaks

Fig. 1 X-ray diffraction patterns after milling for 3 min (A), 21 min (B), 34.5 min (C) and 90 min (D)
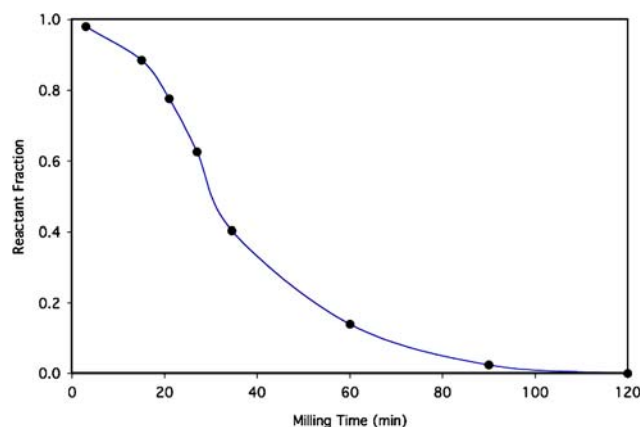
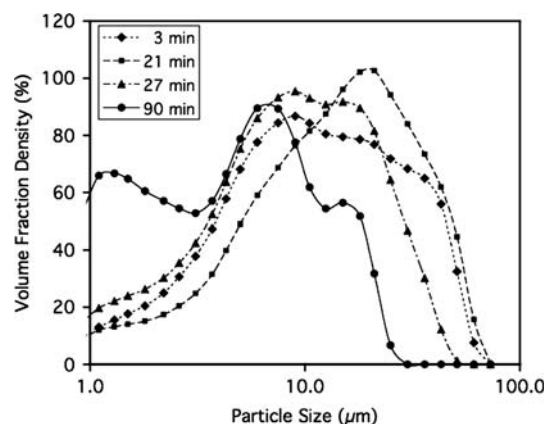Fig. 2 Relative amount of MoS_2 as a function of milling time

Fig. 3 Particle size distribution as a function of milling time

were included in the analysis. The width of the other peaks could not be determined with certainty due to overlap. The estimated particle size and lattice strain are 58 nm and 0.25% after 3 min of milling, 26 nm and 0.5% after 21 min, and 18 nm and 0.6% after 34.5 min. The separation of the two contributions was not possible for longer milling times due to the increasing overlap of the peaks, but the further broadening of the (105) line indicates that the size reduction continues to about 10 nm before all MoS_2 gets transformed by the reaction. The exact values of the crystallite size and strain have to be interpreted with caution due to the anisotropic structure and properties of MoS_2. The diffraction peaks of Al are somewhat narrower, indicating that the grain size of Al is at least twice the size of the MoS_2 crystallites. The larger grain size is anticipated as Al is a soft fcc metal [17]. On the other hand, the freshly produced Mo phase is characterized by very small average grain size (~15 nm) and rather low strain (~0.15%) consistent with the bcc structure and hardness of Mo [18]. The peaks of the Al_2S_3 phase are very broad indicating very small crystallite size, but their intensity is too low for quantitative evaluation.

Laser scattering measures the external size of particles or agglomerates, irrespective to their phase composition and internal structure. As the average diameter of the particles is about 10 μm while the XRD grain size is of the order of 20 nm, a typical particle contains some 10^8 grains. The particle size distribution is shown in Fig. 3 for several milling times (See the Appendix for the exact meaning of the plot). The distributions are trimodal, with small dips at 3.1 μm and 12.5 μm separating fines, medium-size particles and larger agglomerates. The volume fractions of the particles smaller than 3.1 μm and larger than 12.5 μm are shown in Fig. 4 as a function of milling time.

The main change during the first 21 min of milling is agglomeration, as seen both in the formation of large agglomerates and the decreasing fraction of very small particles. As pointed out by Chakurov [19], the formation of agglomerates, that consist of a fine mixture of the reactant phases, is a necessary condition for the initiation of a self-sustaining reaction, as it provides large internal interface area and good heat transfer. If the reaction starts at an interface, it produces sufficient heat to propagate the reaction to neighboring interfaces and eventually leads to self-heating of the entire agglomerate. Initiating the reaction at a loose contact point between two free particles is much more difficult.

Mechanical activation causes agglomeration on the 10 μm scale, while grain size refinement and mixing take place on the 10 nm scale. The combination of these processes, together with the increasing number of lattice defects, may lead to the ignition of MSR. In the
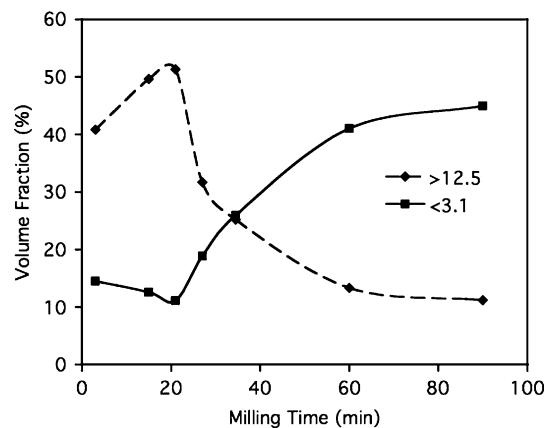

Fig. 4 The relative volume of the largest (larger than 12.5 μm) and smallest (smaller than 3.1 μm) particles as a function of milling time

MoS$_2$–Al system, however, the largest agglomerates—those in which self-heating would be the most effective—begin to break up before the degree of activation is sufficient for the initiation of MSR, probably because the increasingly fine dispersion of MoS$_2$ reduces the adhesion between grains. This change is quite dramatic. After 21 min of milling the largest agglomerates are about 60 μm in diameter, while no particle larger than 40 μm is present after 27 min. It seems that finely distributed MoS$_2$ prevents sufficient agglomeration and consequently the initiation of MSR.

This explanation is consistent with the morphology observed by SEM. At the early stages of the process, a fine dispersion of submicron MoS$_2$ particles forms, as shown by the backscattered electron image of the cross section of a typical particle after 27 min of milling (Fig. 5). The MoS$_2$ particles, appearing bright due to the high atomic number of Mo, are submicron in size. The Al particles are platelets measuring a few microns in diameter. Although the entire particle holds together, the sub-micron grains seem to be packed loosely, preventing the fast propagation of the reaction. Also, the weakly agglomerated particles could break up easily upon continued milling. After 34.5 min of milling, the Mo rich regions are too small to be resolved by backscattered electrons. By that time, the largest particles have broken up and about 50% of the chemical reaction has taken place by localized processes.

The looseness of the agglomeration is also obvious from the secondary electron image taken of particles sprinkled onto conductive paint. Figure 6a shows the structure of the powder after 34.5 min of milling. The larger composite particles are covered with fines, many
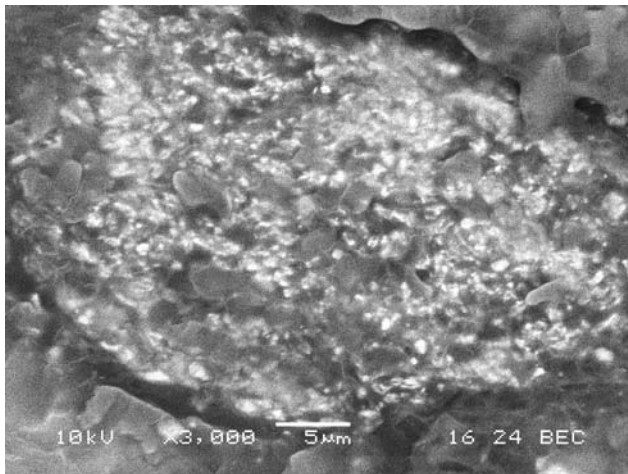
of them showing the typical flaky shape of MoS$_2$ particles. Milling for 90 min visibly increases the amount of fines and the shape of the particles becomes more equiaxed (Fig. 6b). This observation is consistent with the change of the particle size distribution (Fig. 3). At this stage, the reaction is almost complete and the metal phase present is hard Mo rather than Al, explaining the weaker tendency for agglomeration. Work hardening also contributes to the formation of very fine particles.

Thermal stability

Attempts were made to initiate the reduction of MoS$_2$ with Al by heating mechanically activated powder mixtures in a DTA. However, according to XRD (Table 1), the main reaction was oxidation, in spite of flushing the instrument with high purity argon for 2 h before starting the heating program. Although the air sensitivity of the activated powder is anticipated, the degree of oxidation observed in these samples is
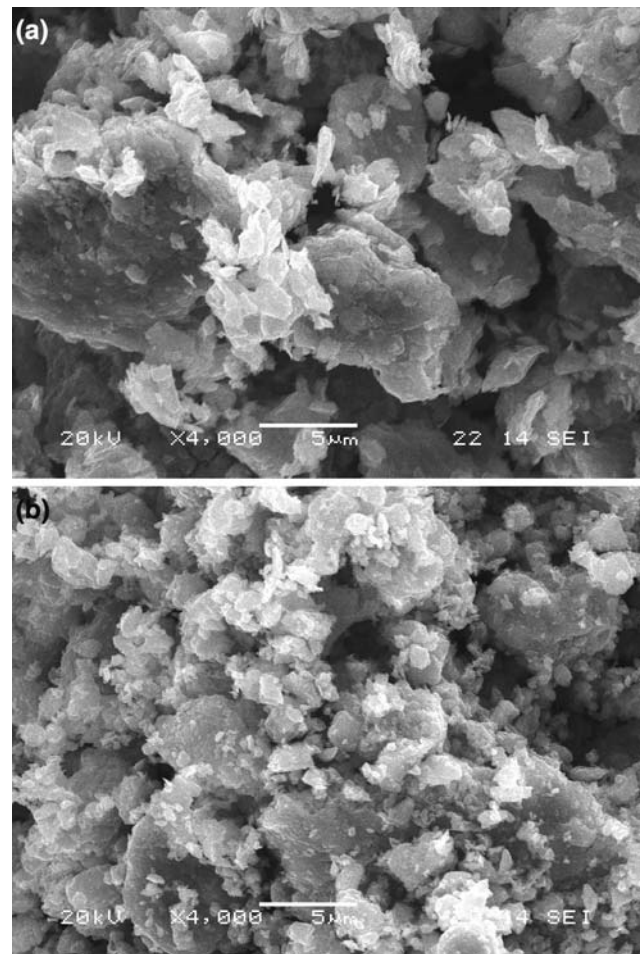

Fig. 5 Backscattered electron image of the cross section of a typical composite particle after 27 min of milling

Fig. 6 Secondary electron image of the powder after 34.5 min (**a**) and 90 min (**b**) of milling

Table 1 Qualitative intensity of the XRD patterns obtained from samples heated to 900 °C in the DTA; (s, m, and w denote strong, medium, and weak diffraction peaks)

Milling time (min)	MoS_2	Al	Mo	Al_2O_3	MoO_2
3	s	S	w	w	–
21	s	W	w	w	–
34.5	m	–	m	–	m
90	w	–	s	–	m

surprisingly high. The intended reaction was easily observed in other systems—e.g. the formation of $MoSi_2$ from a mixture of Mo and Si powders [20]—under very similar conditions.

The DTA measurements were carried out to 900 °C at a heating rate of 20 °C/min in flowing argon. The broad exothermic peak due to oxidation started at 425, 275, and 225 °C for the samples milled for 3, 21 and 34.5 min, respectively. The very high oxygen sensitivity of the powders is consistent with the extremely fine dispersion of the particles. The melting of Al was observed only in the sample milled for 3 min; practically all Al oxidized before reaching the melting point in the samples milled for 21 min and 34.5 min. The Mo fraction found by XRD (Table 1) was formed during milling. Little reflection from Al_2O_3 was detected due to its low crystallinity and low X-ray scattering intensity.

Conclusions

Although the reduction of MoS_2 with Al is a highly exothermic reaction that was expected to progress in the form of a self-sustaining process, ignition could not be achieved by ball milling. It is suggested that the reason is the lubricant property of MoS_2, that prevents the formation of large composite agglomerates. Grains in the existing agglomerates are packed loosely and they start breaking up before the reaction could accelerate. The extreme oxygen sensitivity of the powder is consistent with the low degree of agglomeration.

This results point to the importance of forming well-compacted agglomerate particles, where the abundance of interfaces and good heat transfer allow the escalation of an incipient reaction into a self-sustaining process extending to the entire particle and eventually to the entire volume of the powder charge.

Appendix

The particle size distribution is characterized in Fig. 3 by plotting the volume fraction density (Q_{log}) as a function of the decadic logarithm of the particle diameter (log x.) From this graph, the volume fraction of particles between diameters x_1 and x_2,

$P(x_1 < x < x_2)$, is obtained as the area under the curve between $\log x_1$ and $\log x_2$. If $x_2 - x_1 \ll x_2$,

$$\begin{aligned} P(x_1 < x < x_2) &\approx Q_{log}(\log x_2 - \log x_1) \\ &= Q_{log} \log (x_2/x_1) \end{aligned} \quad \text{(A.1)}$$

Although the proper variable of the horizontal axis is $\log x$, it is usually labeled in terms of diameters. The logarithm is dimensionless, thus both P and Q_{log} can be expressed in percentages.

The quantity most often used to characterize the particle size distribution is the cumulative distribution $F(x)$, defined as the volume fraction occupied by particles smaller than x. If an atom of the sample is chosen at random, $F(x)$ gives the probability that it belongs to a particle smaller than x. As F is an integral quantity, it may hide some fine details of the particle size distribution. Q_{log} relates to F as follows:

The volume fraction of particles between diameters x_1 and x_2 is

$$P(x_1 < x < x_2) = F(x_2) - F(x_1). \quad \text{(A.2)}$$

If $\Delta x = x_2 - x_1 \ll x_2$,

$$P(x_1 < x < x_2) \approx Q(x_2 - x_1) = Q\Delta x, \quad \text{(A.3)}$$

where $Q = dF/dx$ is the volume fraction density. The dimension of Q is 1/length. Q_{log} differs from Q, because its variable is $\log(x)$ rather than x. But Eq. (A.1) and (A.3) provide the same quantity, consequently

$$Q\Delta x = Q_{log} \log(1 + \Delta x/x_1) \approx Q_{log}[\log(e)/x]\,\Delta x. \quad \text{(A.4)}$$

From here,

$$Q_{log} = Qx/\log(e) \approx 2.3x\,Q = 2.3\,x\,dF/dx. \quad \text{(A.5)}$$

References

1. Heinicke G (1984) Tribochemistry. Hanser Publishers, München
2. Avvakumov EG (1986) Mechanical Methods of the Activation of Chemical Processes. Nauka Publishing House, Novosibirsk
3. Suryanarayana C (2001) Prog Mater Sci 46:1
4. McCormick PG (1992) Metall Trans A 23A:1285
5. Takacs L (1993) NanoStruct Mater 2:241
6. Takacs L (1996) J Sol State Chem 125:75
7. Sugamata M, Kaneko J, Higuchi H (1998) Mater Sci Forum 269–272:157
8. McCormick PG (1995) Mater Trans JIM 36:161
9. Tsuzuki T, McCormick PG (2004) J Mater Sci 39:5143
10. Schaffer GB, McCormick PG (1989) Appl Phys Lett 55:45
11. Takacs L (1992) Mater Lett 13:119
12. Takacs L (2002) Prog Mater Sci 47:355
13. Torosyan AR, Martirossyan VG, Karakhanyan SS (1998) Int J Self-Propag High-Temp Synth 7:87
14. Rodrigues JA et al (1991) J Mater Sci Lett 10:819
15. Kubaschewski O, Alcock CB, Spencer PJ (1993) Materials Thermochemistry, 6th ed. Pergamon Press, Oxford
16. Klug HP, Alexander LA (1977) X-Ray Diffraction Procedures for Polycrystalline and Amorphous Materials, 2nd Ed. John Wiley and Sons, New York, p 665
17. Eckert J, Holzer JC, Krill CE, Johnson WL, (1992) J Mater Res 7:1751
18. Fecht HJ, Hellstern E, Fu Z, Johnson WL (1990) Metall Trans A 21A:2333
19. Chakurov Chr, Rusanov V, Koichev J (1987) J Sol State Chem 71:522
20. Takacs L, Soika V, Baláž P (2001) Sol State Ionics 141–142:641